Accurate measurement of uncorrelated energy spread in electron beam

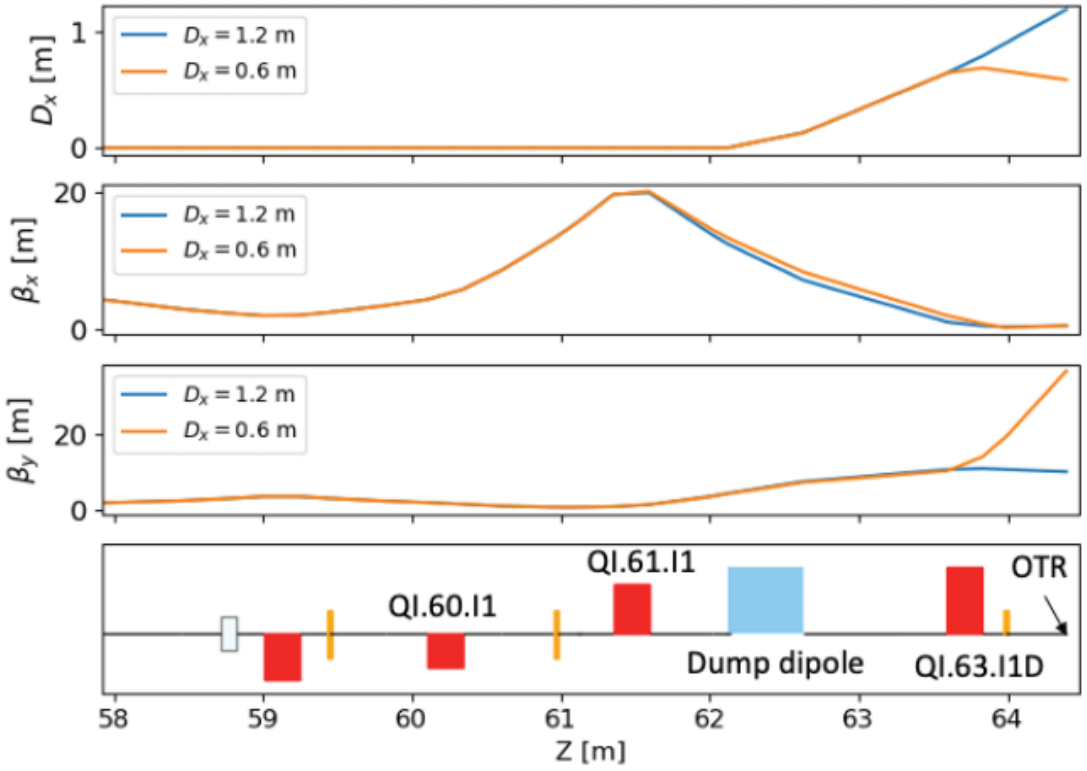

Sergey Tomin, Igor Zagorodnov, Winfried Decking, Nina Golubeva and Matthias Scholz

S2E Meeting
DESY, Hamburg
March 16, 2021

Outline

- Energy spread measured at FERMI and at SwissFEL
- Methods of the measurement at the European XFEL and their analysis
  - Energy scan method
  - Dispersion scan method
  - Impact of systematic and random instrumental errors
- Modelling of the experiments with collective effects and the beam transport
  - Magnetic lattice and its properties
  - Modeling of energy scan method
  - Modeling of dispersion scan method
- Measurements
- Discussion. Intrabeam scattering.
- Summary

Energy spread measured at FERMI

S Di Mitri et al, Experimental evidence of intrabeam scattering in a free-electron laser driver, New J. Phys. 22 (2020) 083053

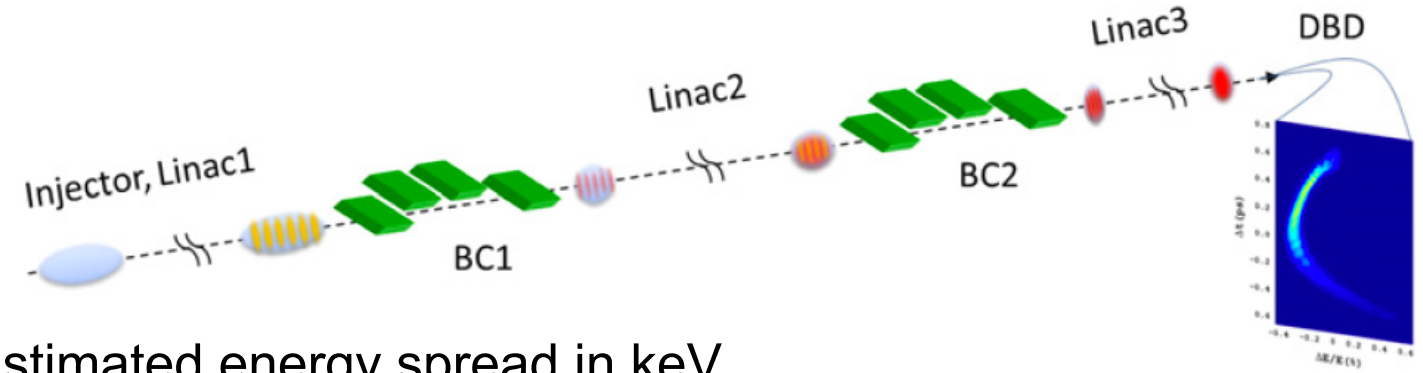

Estimated energy spread in keV

	100 pC	650 pC
With IBS	0.9	2.4
Without IBS	5.5-6.8	4.3

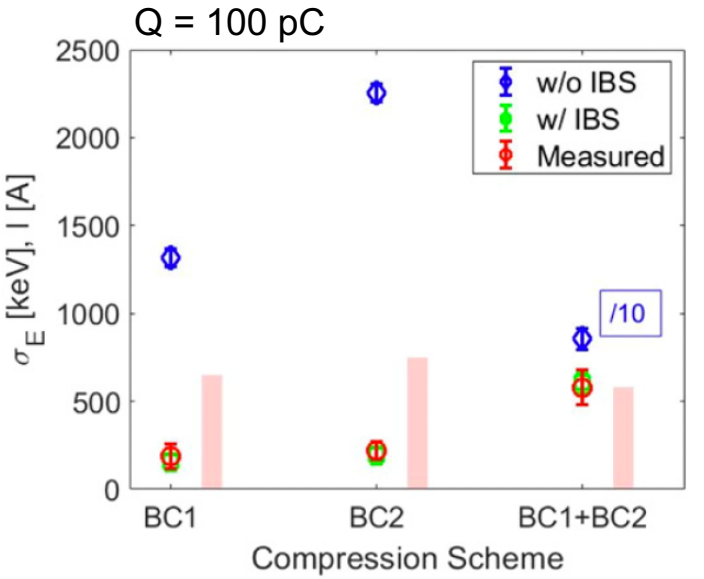

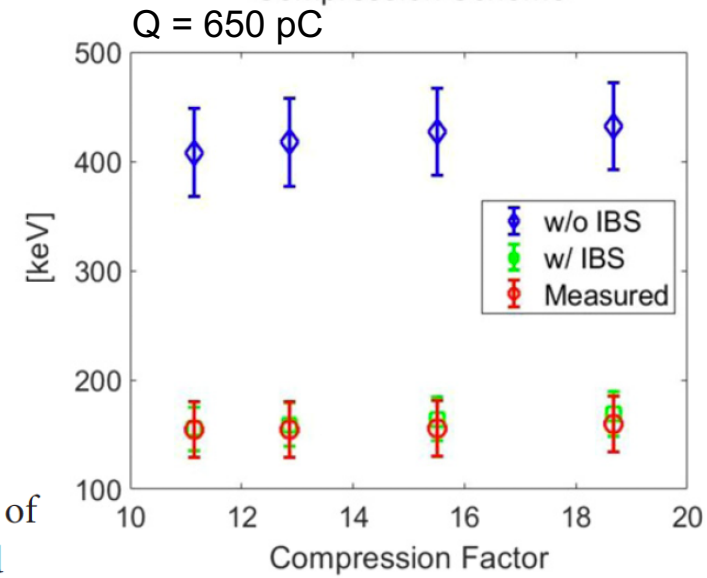

The major uncertainty in our model is the initial value of the uncorrelated energy spread, $\sigma_{E,0}$, i.e., the uncorrelated energy spread at the exit of the linac photo-injector. Since its variation at keV level substantially modifies the model prediction, and since there is no direct measurement of $\sigma_{E,0}$ because of limited resolution, it has been treated in our model as a fitting parameter. That is, while keeping all other machine and beam parameters fixed and in adherence to the experimental settings, we scanned the value of $\sigma_{E,0}$, for the 100 pC and 650 pC bunch charge, in order to obtain a systematic agreement of the measured and the predicted SES over all compression schemes and compression factors. This procedure reproduces

Energy spread measured at SwissFEL

E Prat et al, High-resolution dispersion-based measurement of theelectron beam energy spread, PRAB 23 (2020) 090701

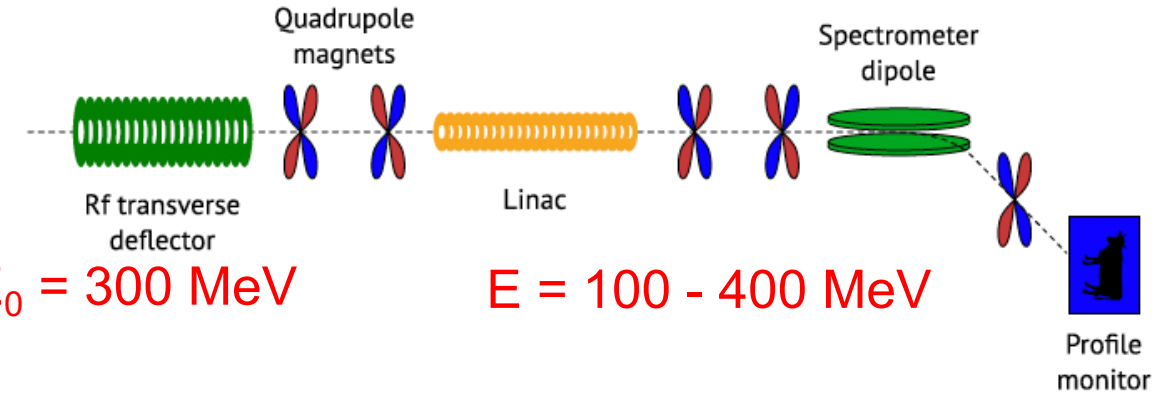

E_0 = 300 MeV E = 100 - 400 MeV

$$\sigma_M^2 = \sigma_R^2 + \frac{E_0}{E}\sigma_B^2 + \frac{D^2}{E^2}\sigma_{EI}^2$$

$$\sigma_{EI}^2 = \sigma_E^2 + (ekV)^2\sigma_I^2$$

$$\sigma_B^2 = \frac{\beta_x \epsilon_n}{\gamma_0} \qquad \sigma_I^2 = \frac{\epsilon_n \beta_y^0}{\gamma_0}$$

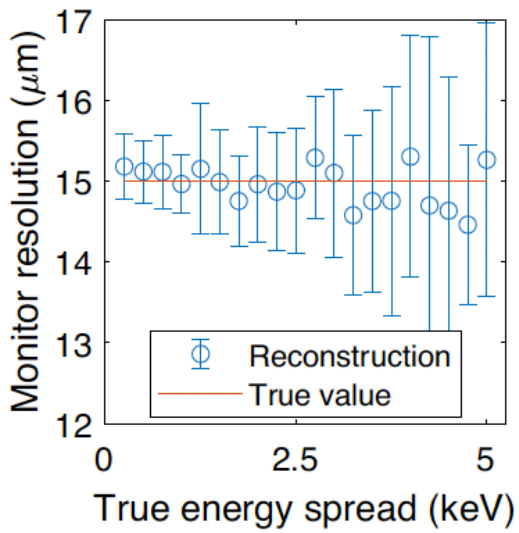

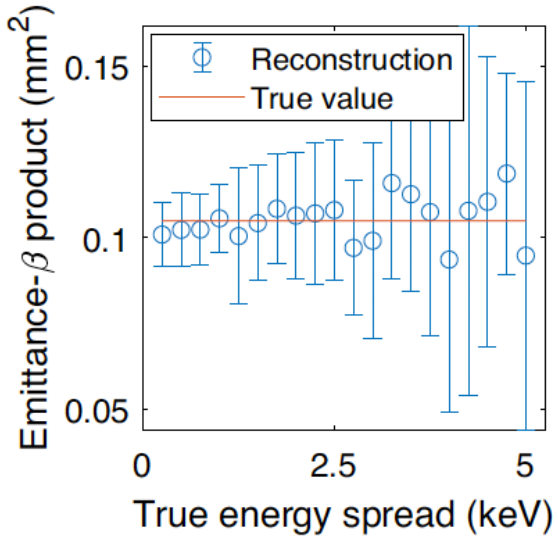

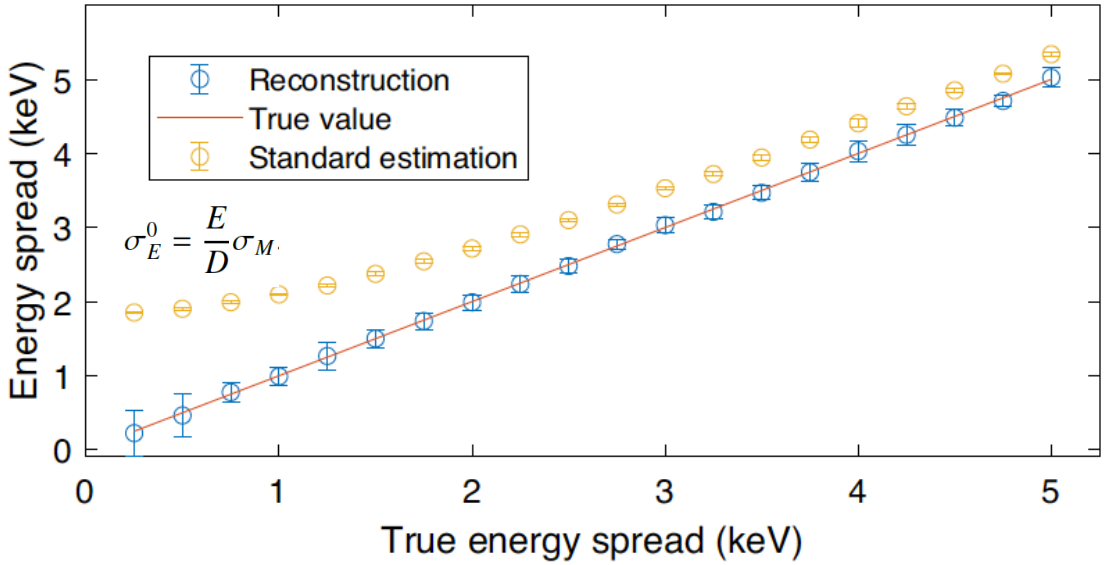

Energy spread measured at SwissFEL

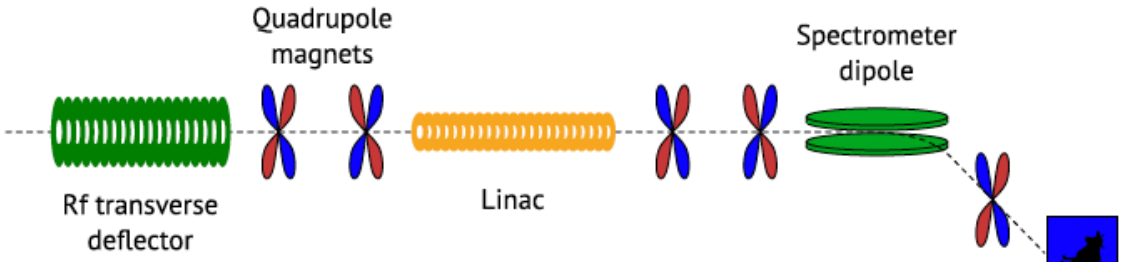

E_0 = 300 MeV

E = 100 - 430 MeV

$$\sigma_E^0 = \frac{E}{D}\sigma_M$$

$$\sigma_{EI}^2 = \sigma_E^2 + (ekV)^2\sigma_I^2$$

Estimated energy spread in keV

	10 pC	200 pC
Direct measurement	7.1 ± 0.6	15.1 ± 0.6
With TDS induced	6.5 ± 0.3	15 ± 0.3
Without TDS induces	6.3	**14.8**

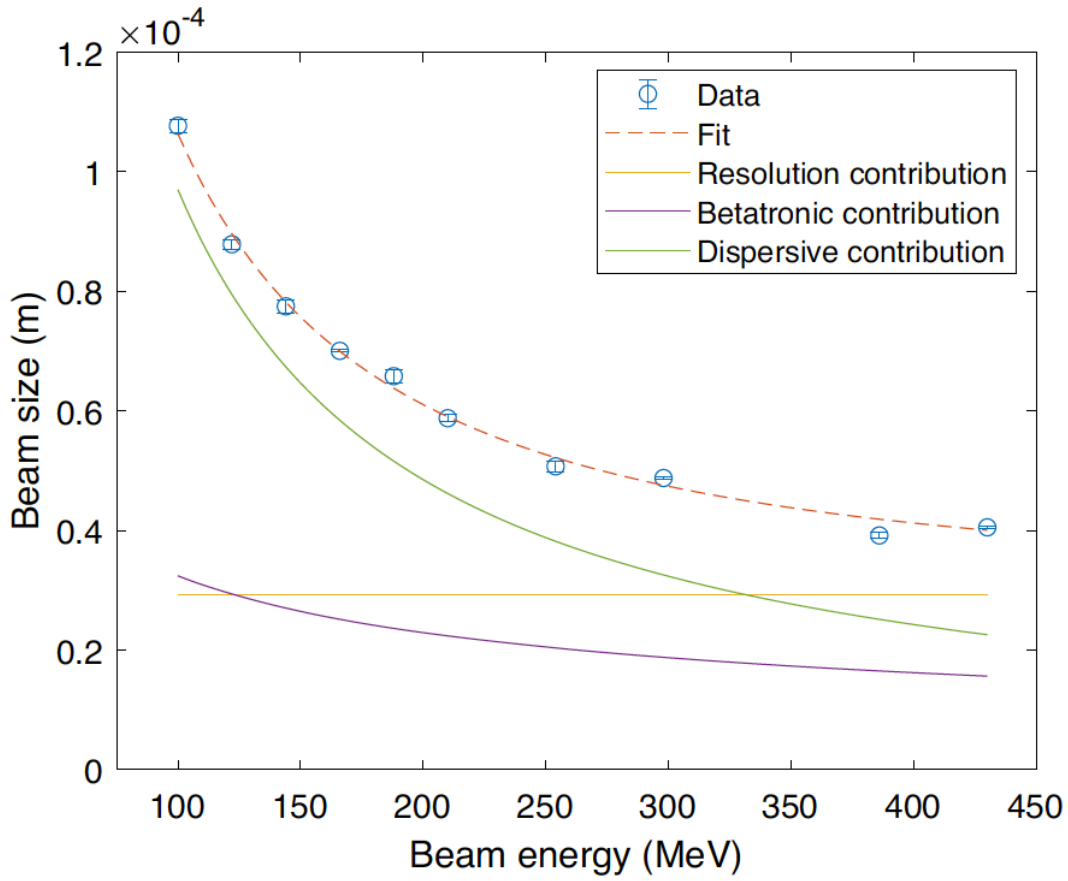

FIG. 7. Measured beam sizes at the profile monitor and corresponding fits for the different contributions for a beam charge of 10 pC. The reconstructed energy spread is 6.5 keV.

Energy scan method at the European XFEL

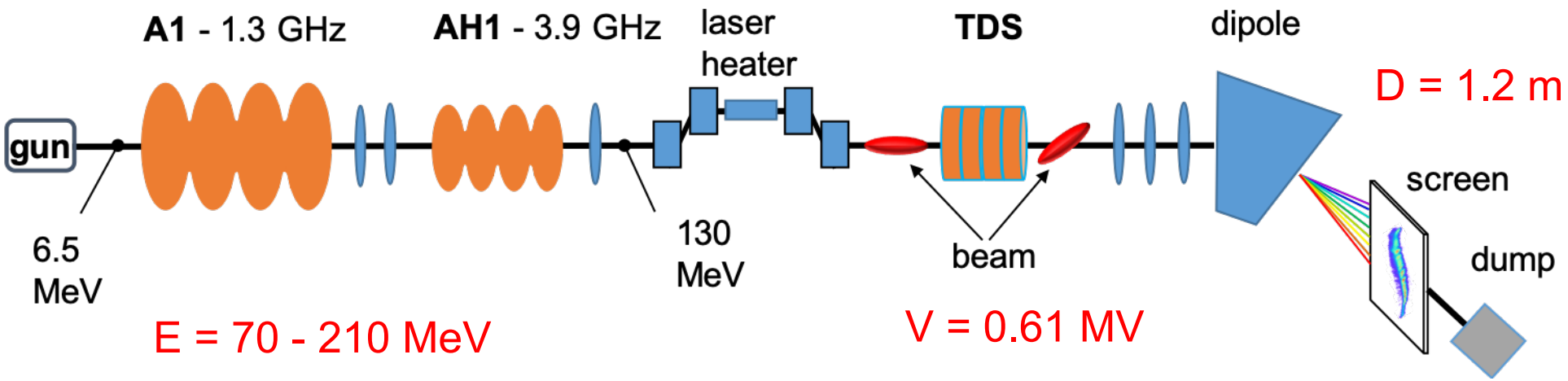

E = 70 - 210 MeV

E_0 = 130 MeV

V = 0.61 MV

$$\sigma_M^2 = \sigma_R^2 + \frac{E_0}{E}\sigma_B^2 + \frac{D^2}{E^2}\sigma_E^2 + \frac{(DekV)^2 E_0}{E^3}\sigma_I^2,$$

$$\sigma_B^2 = \frac{\beta_x \epsilon_n}{\gamma_0}, \quad \sigma_I^2 = \frac{\epsilon_n(\beta_y^0 + 0.25L^2\gamma_y^0 - L\alpha_y^0)}{\gamma_0},$$

Distance between pixels on the screen:
energy axis - 13.7369μm
time axis - 11.1756 μm

Energy scan method at the European XFEL

TABLE I: Simulation parameters.

parameter	Units	Value
OTR resolution, σ_R	μm	28
Normalized emittance, ϵ_n	μm	0.4
Reference optical β-function at OTR , β_x^0	m	0.6
Reference dispersion, D_0	m	1.2
Optical α-function at TDS, β_y^0	m	4.3
Optical β-functionr at TDS, α_y^0		1.9
Wave number of TDS, k	1/m	58.7
Length of TDS, L	m	0.7
Reference voltage of TDS, V_0	MV	0.61
Reference energy, E_0	MeV	130

If we keep the voltage of the deflector constant and change only the beam energies than we can fit the measurements to Eq.(1) in hope to reconstruct all coefficients of this polynomial. We simulated with Eq.(1) a measurement of the beam size σ_M with constant TDS voltage V_0 and the beam energy changing between 90 and 190 MeV with step of 10 MeV. At each beam energy we simulate 30 measurements of the beam size σ_M with random error of 2%. We consider the slice energy spread between 0.5 and 7 keV. In the fit we used the simplex search method of Lagarias et al [6].

From numerical experiment we have found that the rms error of the reconstruction of energy spread is larger than 2 keV. Under the rms error of reconstruction in the paper we mean the value defined as

$$\Delta_{\sigma_E} = \sqrt{\frac{1}{N}\sum_{i=1}^{N}(\sigma_E - \sigma_E^0)^2}, \tag{4}$$

where N is the number of shots (reconstructions), σ_E is the energy spread obtained

Energy scan method at the European XFEL

$$\sigma_M^2 = \sigma_R^2 + \frac{E_0}{E}\sigma_B^2 + \frac{D^2}{E^2}\sigma_E^2 + \frac{(DekV)^2 E_0}{E^3}\sigma_I^2,$$

In order to reduce the error we can do an additional scan with different deflector voltages to estimate the last term in Eq.(1). With this estimation we reduce the error of the reconstruction. However, we will not analyze this approach here and suggest below another technique to reduce the order of the polynomial and to increase the accuracy of the reconstruction of the polynomial coefficients.

It can be achieved if we will keep constant not the voltage V but the streaking

$$S_0 = \sqrt{\beta_y \beta_y^0}\sin(\Delta\mu_y)K_0, \qquad K_0 = \frac{eV_0 k}{E_0},$$

Energy scan method at the European XFEL

In the following we adjust the voltage of TDS proportionally to the beam energy:

$$V(E) = \frac{V_0}{E_0} E. \qquad (6)$$

If we put Eq.(6) in Eq.(1) then we reduce the order of the polynomial from the third to the second one:

$$\sigma_M^2 = \sigma_R^2 + \frac{E_0}{E}\sigma_{BI}^2 + \frac{D^2}{E^2}\sigma_E^2, \quad \sigma_{BI}^2 = \sigma_B^2 + (DK_0\sigma_I)^2. \qquad (7)$$

Energy scan method at the European XFEL

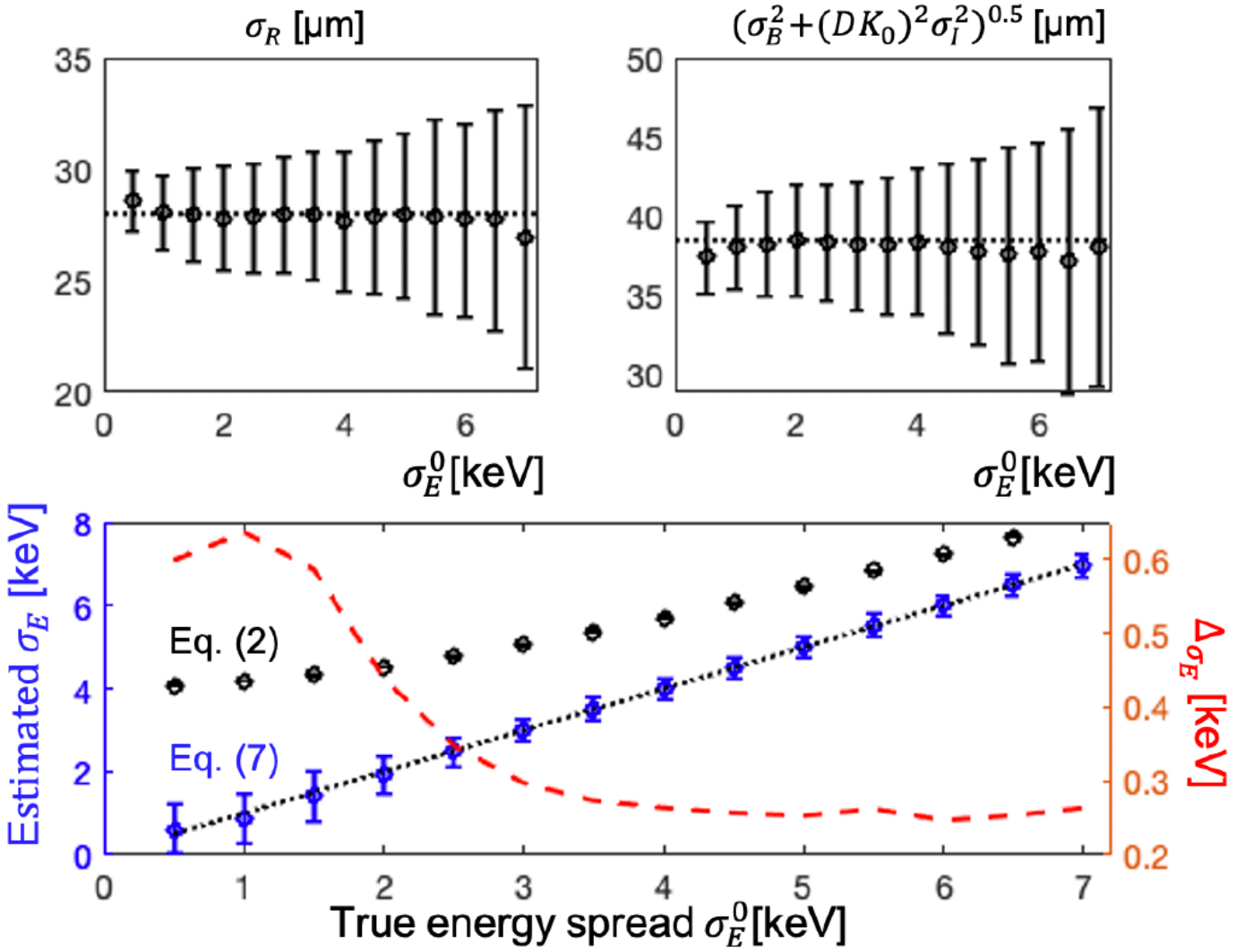

E_0 = 130 MeV

E = 90 - 190 MeV

$$\sigma_M^2 = \sigma_R^2 + \frac{E_0}{E}\sigma_{BI}^2 + \frac{D^2}{E^2}\sigma_E^2$$

$$\sigma_{BI}^2 = \sigma_B^2 + (DK_0\sigma_I)^2.$$

$$\sigma_E^0 = \frac{E}{D}\sigma_M.$$

- Conditions at different energies
  - Constant emittance
  - Constant optical functions
  - The same slice is measured
  - Constant slice energy spread

Dispersion scan method at the European XFEL

In this section we present another method which use constant beam energy E_0 and avoids above described difficulties. The method shows much better resolution theoretically and it is easy to use experimentally.

We have developed a special optics described in the next section. Using only few quadrupoles between TDS and the OTR screen we are able to change the dispersion D at the OTR position keeping β_x -function constant with only moderate changes in β_y-function and in the streaking S.

$$\sigma_M^2 = \sigma_R^2 + \sigma_B^2 + \frac{D^2}{E_0^2}\sigma_{EI}^2 \qquad \sigma_{EI}^2 = \sigma_E^2 + (ekV)^2\sigma_I^2$$

Dispersion scan method at the European XFEL

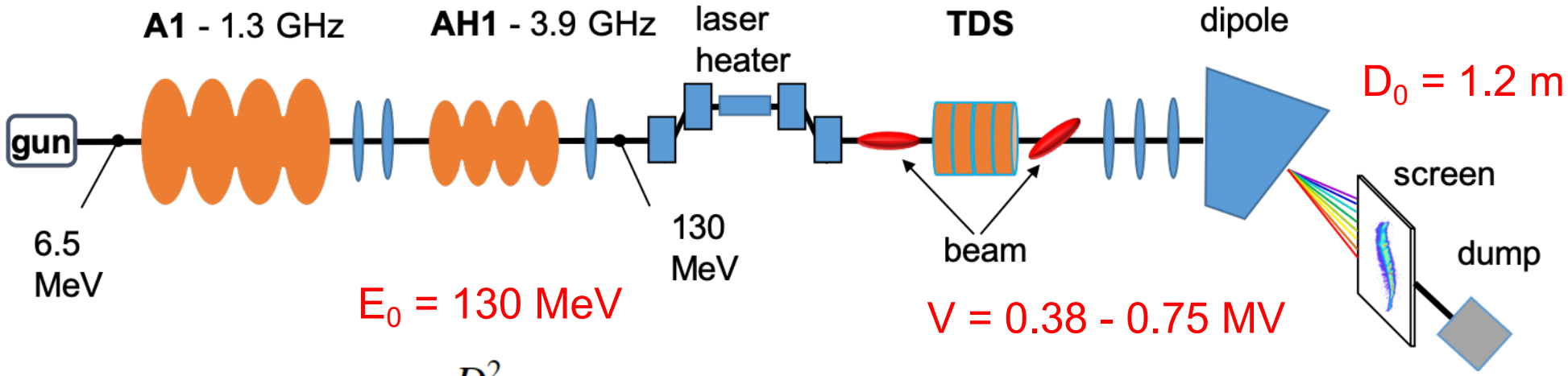

$$\sigma_M^2 = \sigma_R^2 + \sigma_B^2 + \frac{D^2}{E_0^2}\sigma_{EI}^2 \qquad \sigma_{EI}^2 = \sigma_E^2 + (ekV)^2\sigma_I^2$$

We start with changing of TDS voltage V and fit the measured slice size σ_M to the quadratic polynomial:

$$\sigma_M^2 = A_V + B_V V^2. \qquad (8)$$

During the scan we keep the dispersion at constant value D_0.

Dispersion scan method at the European XFEL

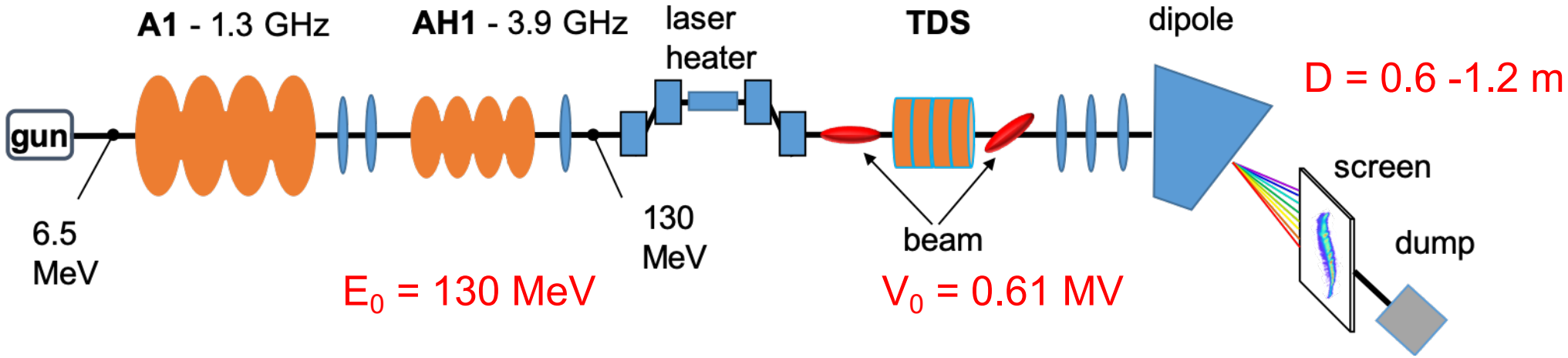

$$\sigma_M^2 = \sigma_R^2 + \sigma_B^2 + \frac{D^2}{E_0^2}\sigma_{EI}^2 \qquad \sigma_{EI}^2 = \sigma_E^2 + (ekV)^2\sigma_I^2$$

At the second step we keep constant the TDS voltage at V_0 and change the dispersion D. We fit the measured slice size σ_M to the quadratic polynomial:

$$\sigma_M^2 = A_D + B_D D^2. \qquad (9)$$

Dispersion scan method at the European XFEL

After these two fits we are able to find out all terms of Eq.(1):

$$\sigma_E = \frac{E_0}{D_0}\sqrt{A_D - A_V}, \quad \sigma_I = \frac{E_0}{D_0 ek}\sqrt{B_V}, \tag{10}$$
$$\sigma_B = \sqrt{B_\beta \beta_x^0}, \quad \sigma_R = \sqrt{A_D - \sigma_B^2},$$

where

$$B_\beta = \sigma_I^2(\beta_y^0 + 0.25L^2\gamma_y^0 - L\alpha_y^0)^{-1}. \tag{11}$$

Eq. (11) calculates the coefficient B_β from the results of the TDS voltage scan, Eq. (8) . Otherwise, if we had measured the slice emittance ϵ_n independently, then we can use more accurate estimation of B_β through the relation $B_\beta = \epsilon_n/\gamma_0$. For example, we can estimate B_β (or emittance ϵ_n) changing only β_x function at the OTR screen position and keeping the dispersion D constant and fitting the measured slice size σ_M to the linear polynomial:

$$\sigma_M^2 = A_\beta + B_\beta \beta_x. \tag{12}$$

$$\sigma_M^2 = \sigma_R^2 + \sigma_B^2 + \frac{D^2}{E_0^2}\sigma_{EI}^2$$

$$\sigma_{EI}^2 = \sigma_E^2 + (ekV)^2\sigma_I^2$$

Dispersion scan method at the European XFEL

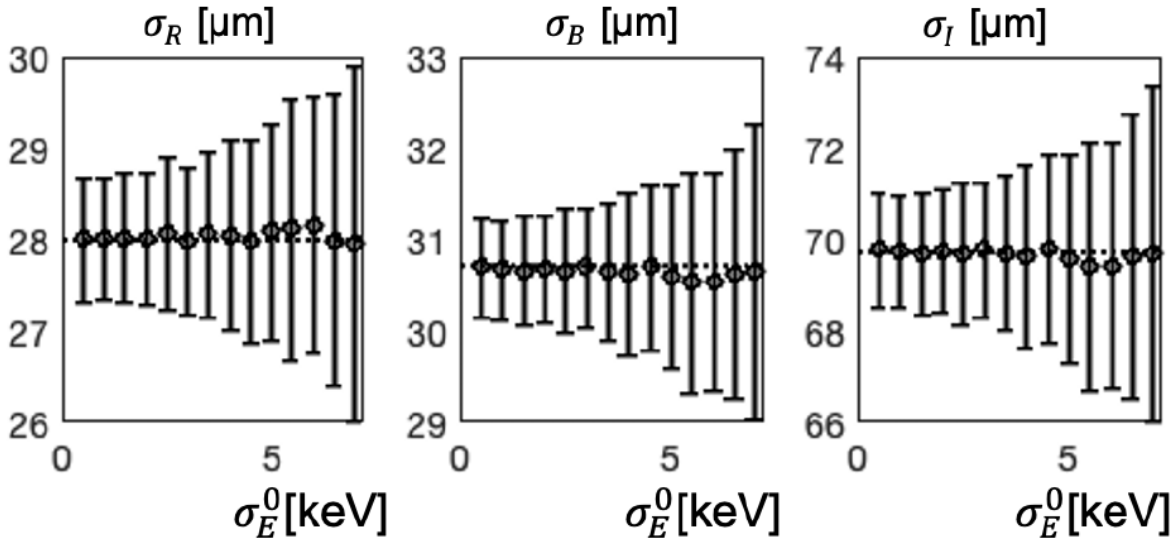

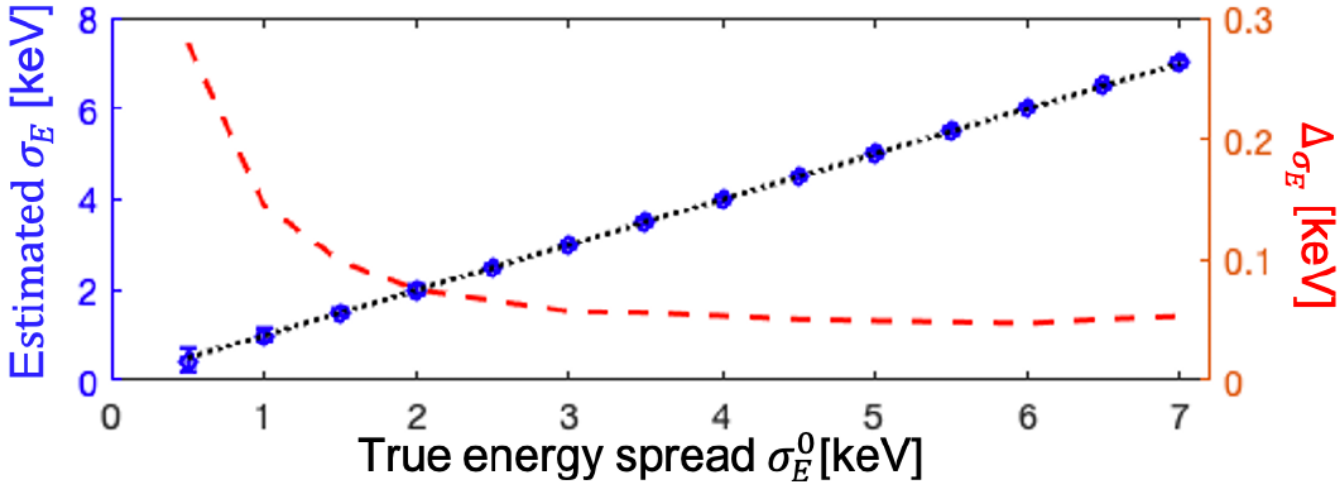

We simulated with Eq. (1) the measurement of the beam size σ_M for two scans as given by Eqs.(8)-(11). For the dispersion scan we used the values of 0.6, 0.8, 1.0 and 1.2 meters. For the TDS voltage scan we used values 0.38, 0.47, 0.56, 0.65 and 0.75 MV. We used the same errors and the reconstruction algorithm as in the previous examples. The results of the reconstruction are shown in Fig. 4 and the error of the reconstruction of energy spread is smaller than 0.1 keV at the energy spread of 6 keV.

$$\sigma_M^2 = \sigma_R^2 + \sigma_B^2 + \frac{D^2}{E_0^2}\sigma_{EI}^2$$

$$\sigma_{EI}^2 = \sigma_E^2 + (ekV)^2\sigma_I^2$$

Impact of systematic and random instrumental errors

$$\sigma_M^2 = A_V + B_V V^2$$

$$\sigma_M^2 = A_D + B_D D^2$$

$$\Rightarrow \quad \sigma_E = \frac{E_0}{D_0}\sqrt{A_D - A_V}$$

If the errors are systematic with the same sign then the reconstruction of energy spread only weakly affected by them. Indeed, we calculate energy spread by Eq. (10) and use only the constant terms A_D and A_V. If we suggest that during the TDS voltage scan we set the voltage with the same negative error, for example it is 10 %, then it has only impact on coefficient B_V which in this case will be increased by factor 0.9^{-2}, but the constant term A_V is not changed. The same is true for the impact of the systematic error in the dispersion D during the dispersion scan.

Dispersion scan method at the European XFEL

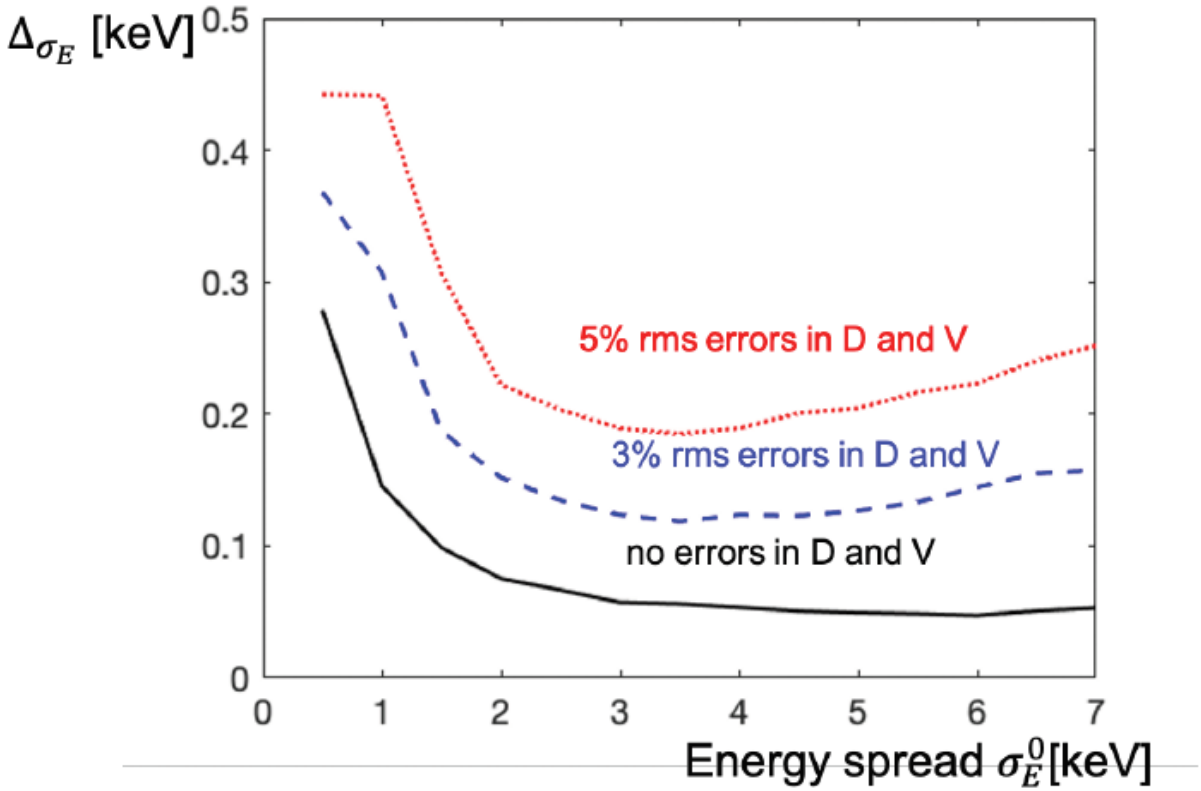

FIG. 4: Impact of instrumental errors in setup of voltage and dispersion on the reconstruction error from dispersion scan method.

Magnetic lattice and its properties

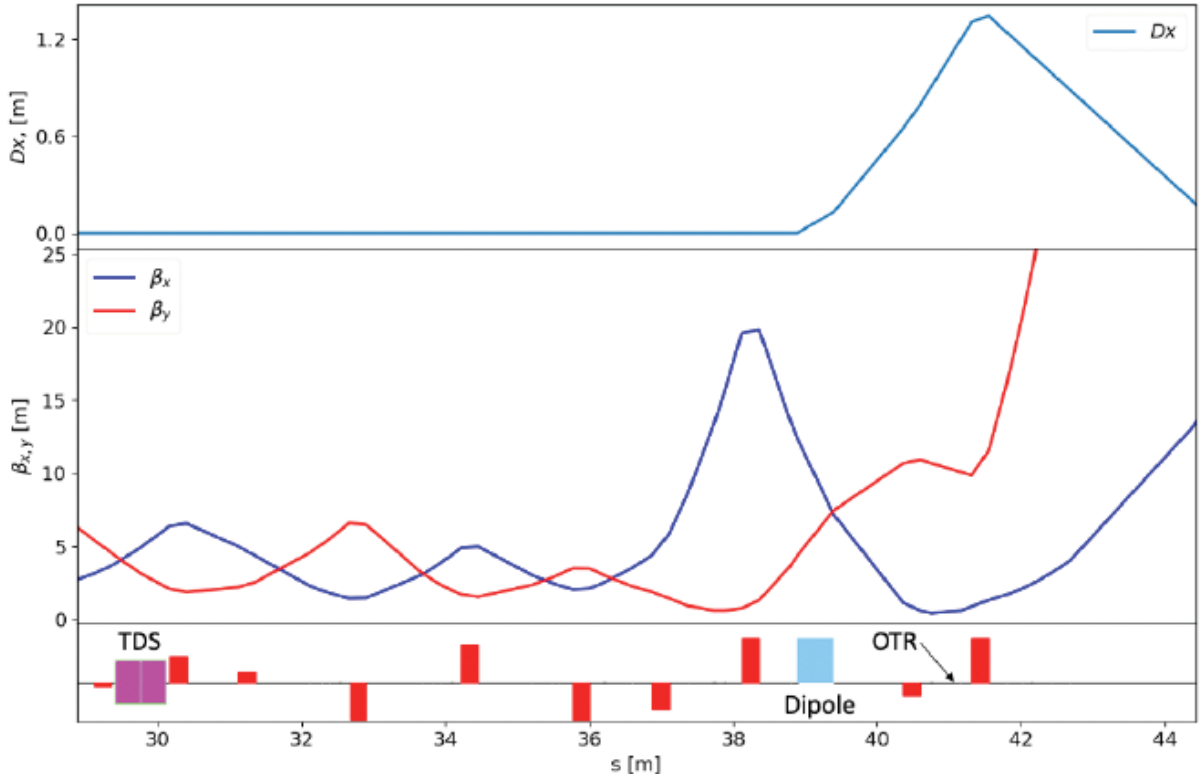

TABLE II: Optics properties not listed in Table I.

parameter	Units	Value
Optical parameters at TDS beginning, α_y/β_y	-/m	1.9/4.3
Optical β-parameters at OTR, $\beta_x/$	m	0.6
Phase advance between TDS and OTR, $\Delta\phi_x/\Delta\phi_y$	deg	260 / 282
$R_{3,4}$ between TDS and OTR		-5.5
Optical β-parameters at matching point, β_x/β_y	m	3.13 / 5.41
Optical α-parameters at matching point, α_x/α_y		-0.92/ 1.73

Magnetic lattice and its properties

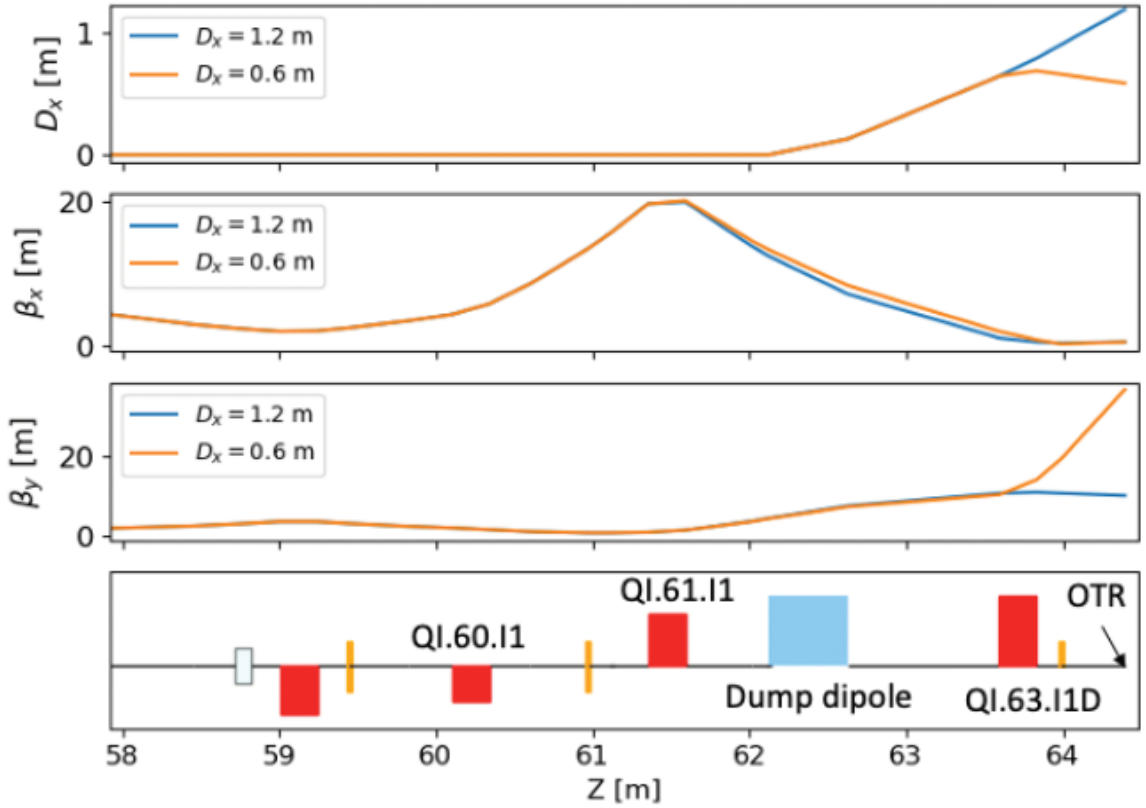

- Only there quads are used to change the dispersion at the screen
- The horizontal beta-function at the screen is constant

FIG. 6: Changes of the twiss parameters in the dump section during dispersion scan.

Modelling of energy scan method

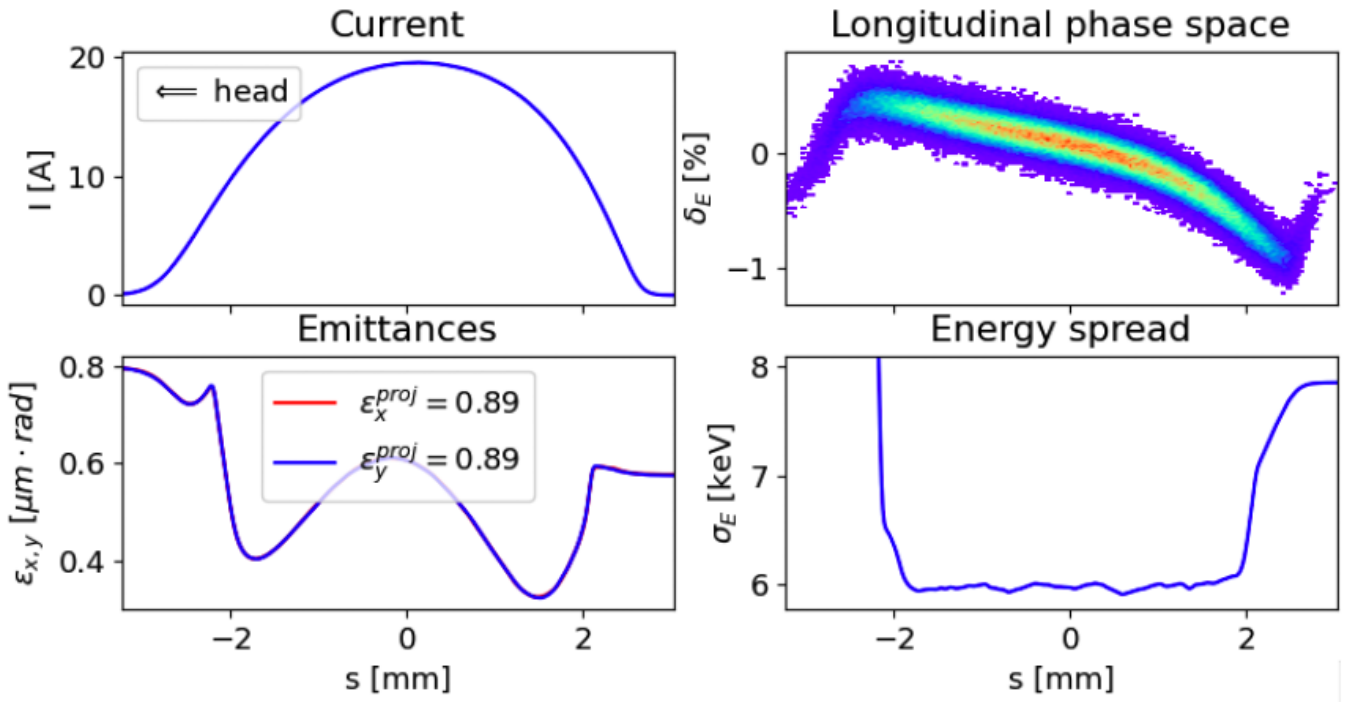

FIG. 8: Electron beam distribution after the gun used in the modeling.

- The energy spread is increased from 0.6 keV to approx. 6 keV with random generator at position z=3.2 meters after the cathode

Modelling of energy scan method

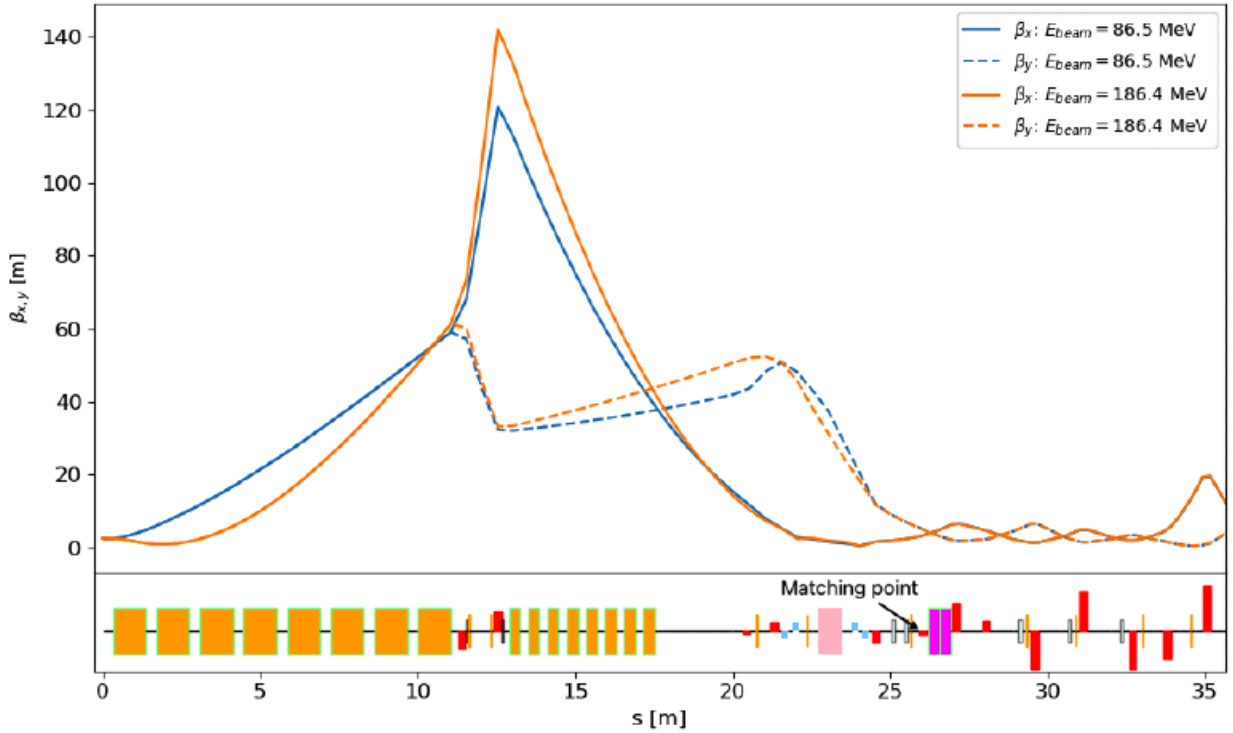

- The RF focusing in A1 depends on energy
- Matching to the optics is required
- The slice emittance changes
- The energy spread due to space charge and IBS changes

FIG. 9: β-functions for lowest and highest energy with space charge effect with taking into account SC effect and RF focusing.

Modelling of energy scan method

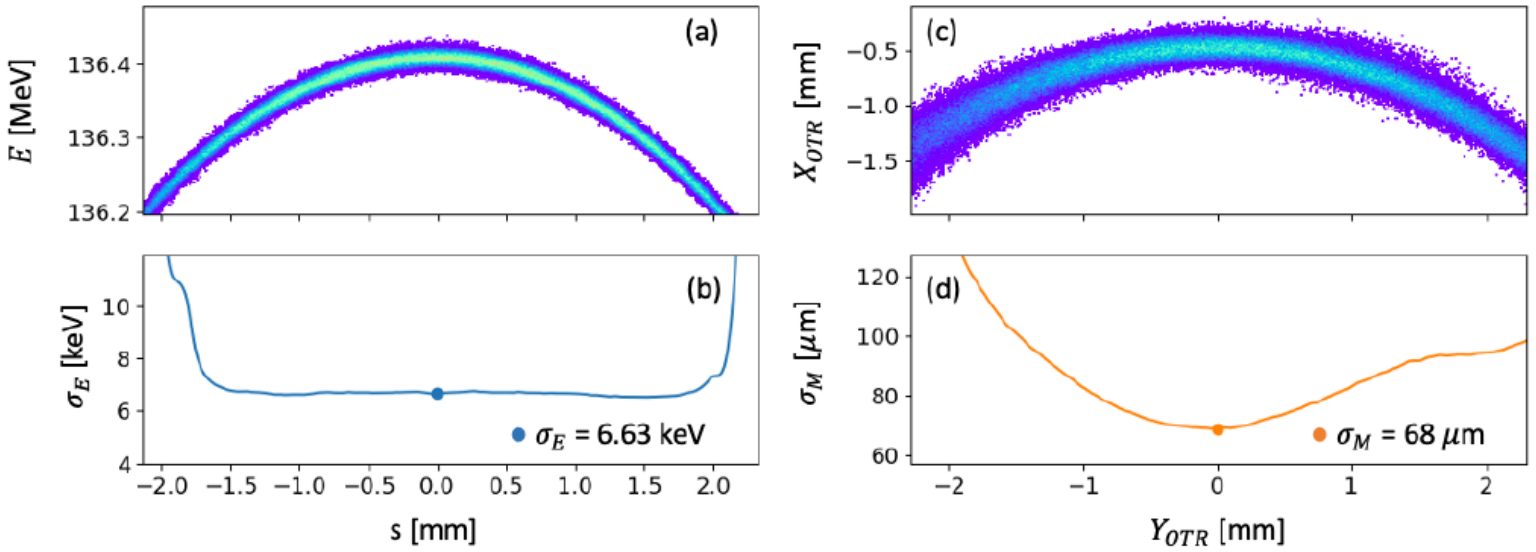

- R51 and R52 increase width of the slices on the screen for the slices outside of the extremum

FIG. 10: Some details of longitudinal beam dynamics for the beam energy 136 MeV. **a)** The LPS beam distribution in front of dump magnet, **b)** slice energy spread of the beam in front of dump magnet, **c)** the beam image on the OTR screen and **d)** horizontal slice beam size on the OTR screen.

Modelling of energy scan method

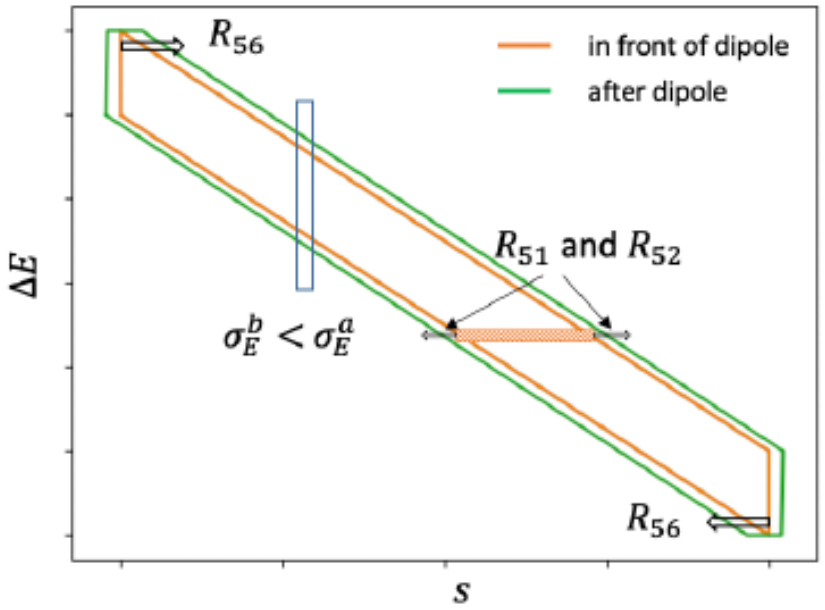

- R51 and R52 increase width of the slices on the screen for the slices outside of the extremum

FIG. 7: LPS dynamics in the dump section. Orange line represents the LPS of the chirped beam before dipole and green line represents LPS of the same beam after the dipole. Expansion in the longitudinal direction occurs due to coupling between horizontal and longitudinal planes (R_{51} and R_{52}).

Modelling of energy scan method

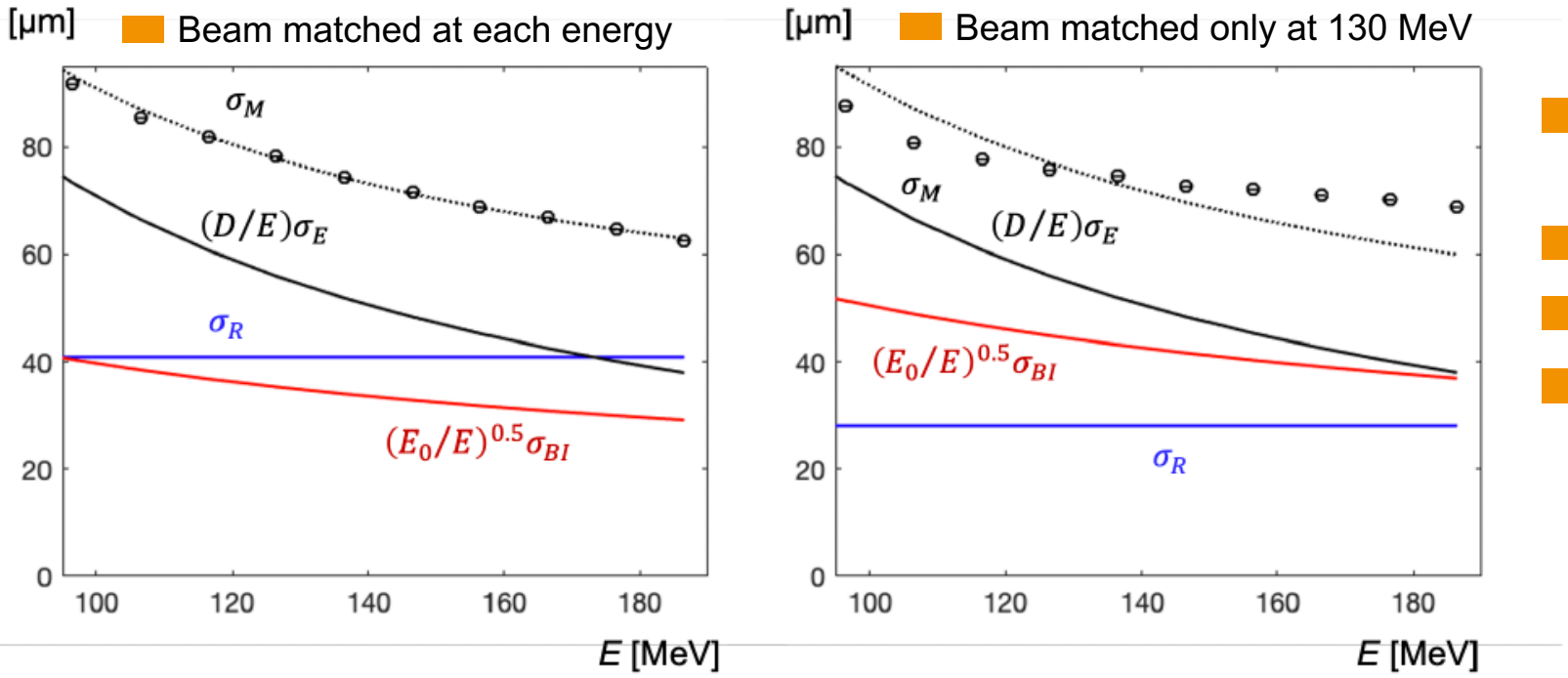

- The RF focusing in A1 depends on energy
- Matching to the optics is required
- The slice emittance changes
- IBS is not included

FIG. 11: The left plot shows the results of reconstruction for the matched beam. The right plot shows only comparison of the measurements of the energy scan (dots with error bars) with the values calculated from the "true" data. The reconstruction for the data in right plot is impossible.

Modelling of energy scan method

TABLE III: The true and the reconstructed data from the beam dynamics simulations at the reference energy $E_0 = 130$ MeV.

Parameter	σ_E	σ_I	σ_B	σ_R	ϵ_n
Units	keV	μm	μm	μm	μm
True values	5.90	80.3	35.4	28	0.53
Energy scan method	5.89			41	
Dispersion scan method	5.97	81.8	36.0	26.4	0.55

Modelling of dispersion scan method

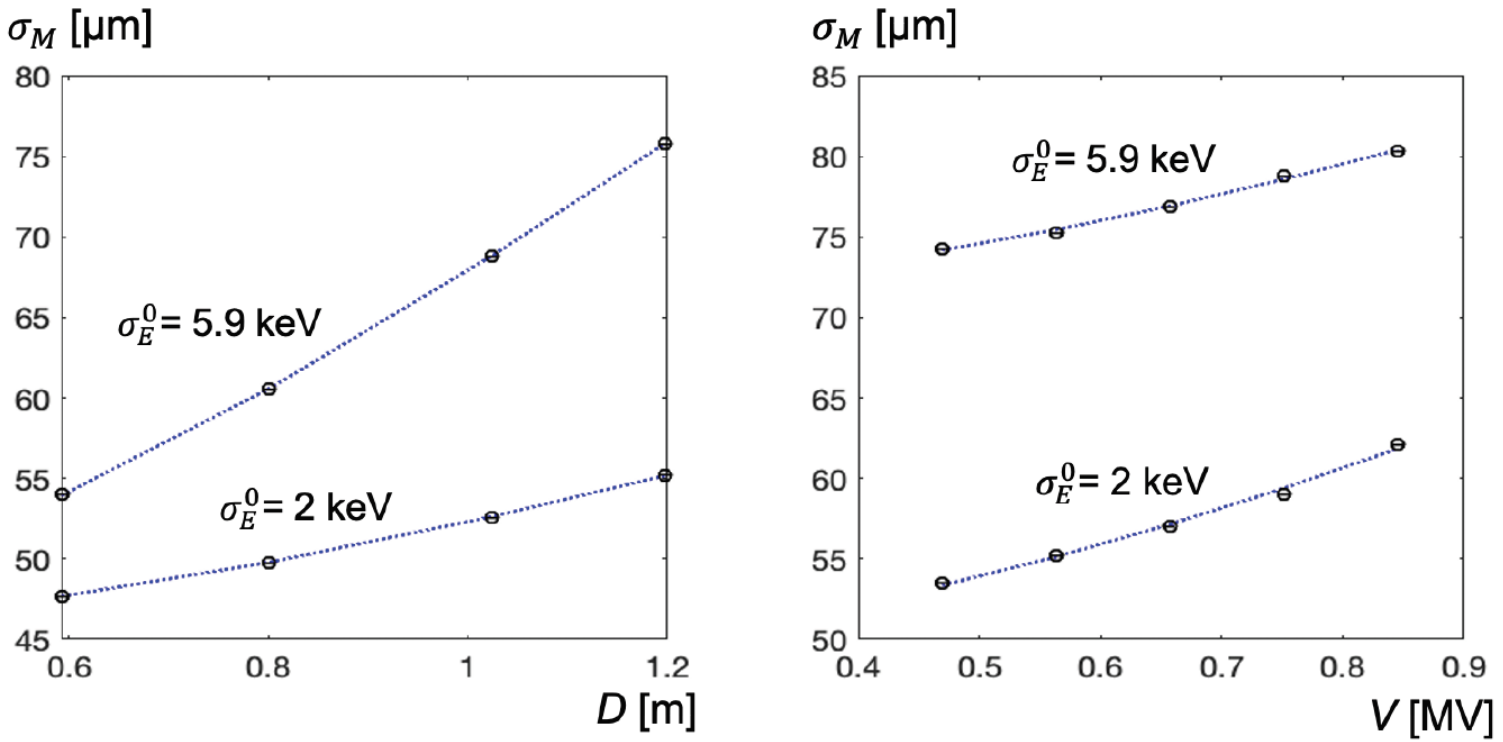

FIG. 12: Beam size changes during dispersion scan and TDS voltage scan. Blue dashed line is obtained from the numerical fit.

Measurement with dispersion scan method

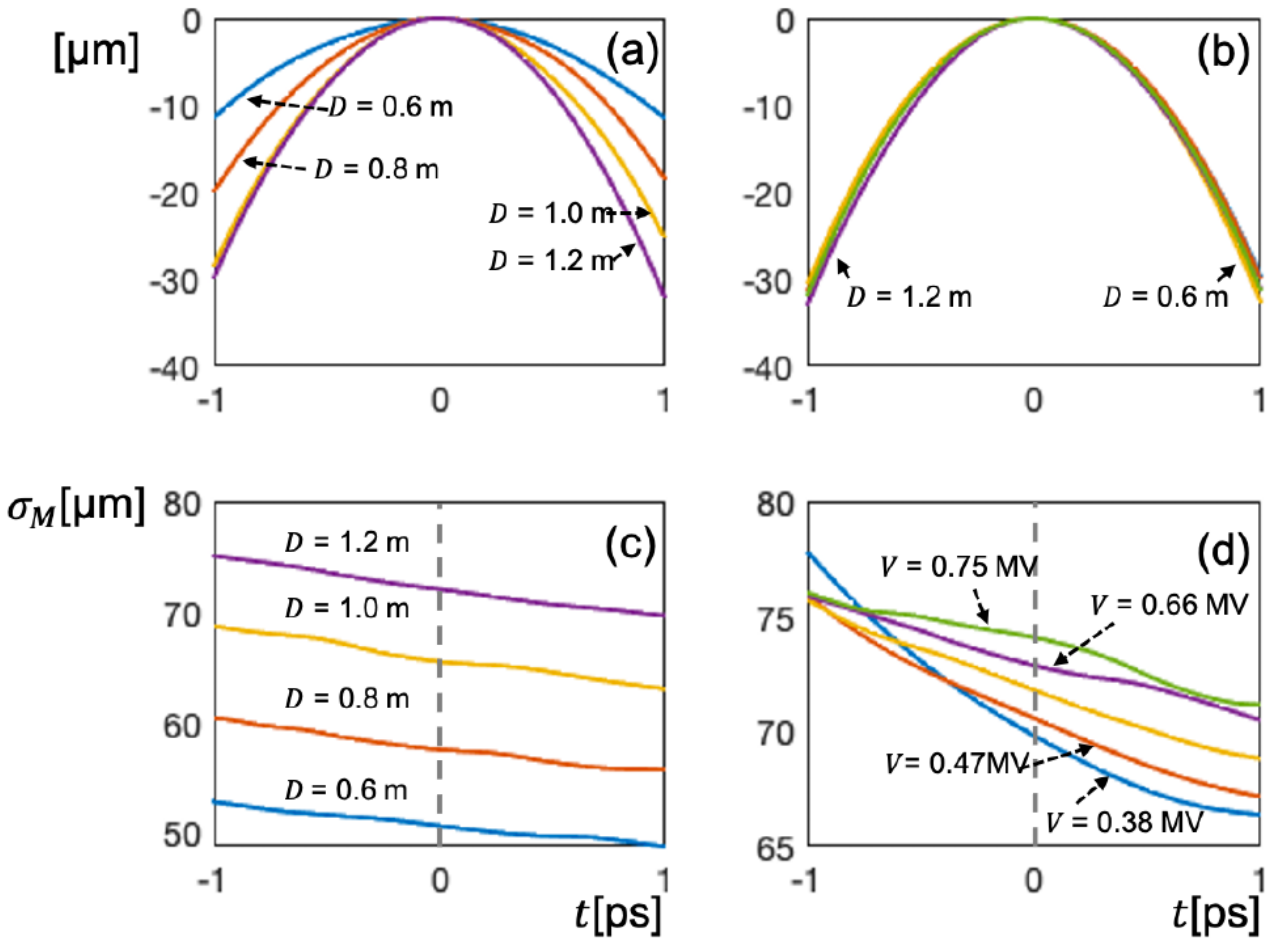

FIG. 13: Measured curves with the dispersion scan method. (a) Mean vertical position of the slices on the screen along the bunch for different dispersion values. (b) Mean vertical position of the slices on the screen along the bunch for different TDS voltages. (c) Vertical size of the slices on the screen along the bunch for different dispersion values. (b) Vertical size of the slices on the screen along the bunch for different TDS voltages. The gray dotted lines present the position of the reference slice.

TABLE IV: Two first rows show the beam sizes measured at different TDS voltages. The last two rows present the beam sizes measured at different dispersion values.

V	MV	0.375	0.469	0.563	0.657	0.751
σ_M	μm	69.87 ± 0.12	70.64 ± 0.10	71.86 ± 0.13	72.85 ± 0.17	74.12 ± 0.14
D	m	0.578	0.789	1.006	1.181	
σ_M	μm	50.62 ± 0.08	57.49 ± 0.09	65.43 ± 0.1	72.05 ± 0.1	

Measurement with dispersion scan method

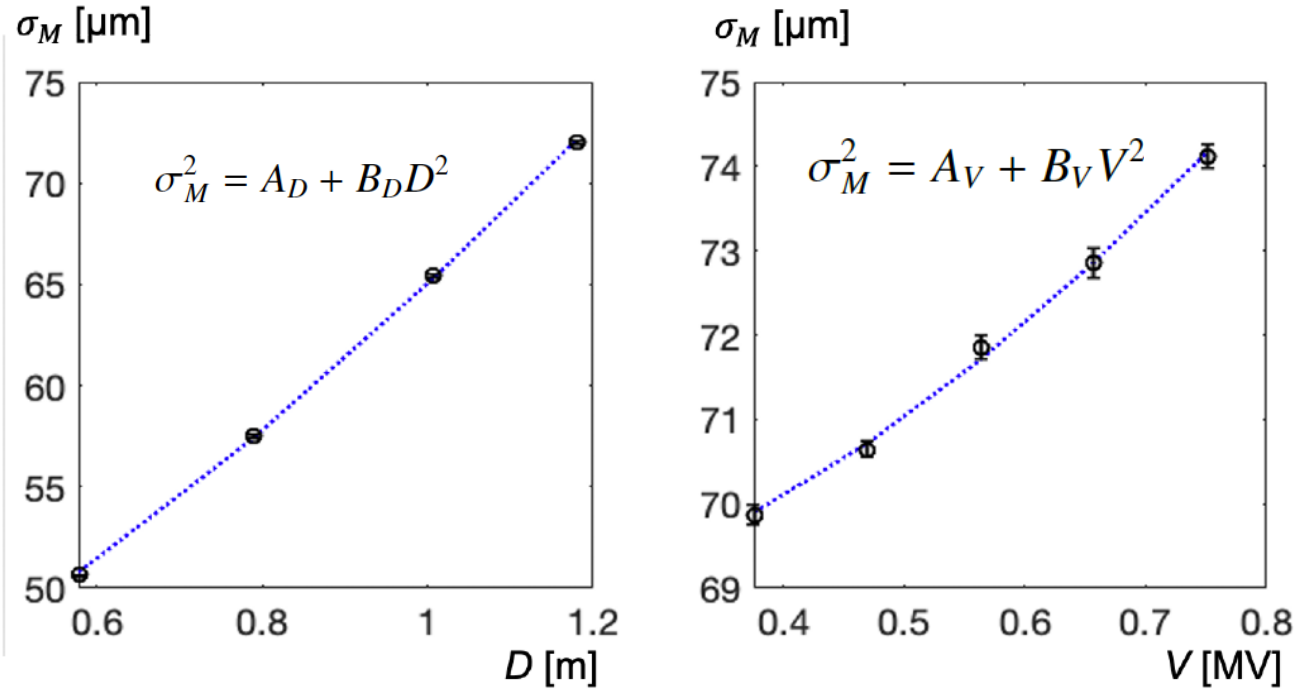

A_V	B_V	A_D	B_D
m^2	m^2/MV^2	m^2	
4.68e-9	1.45e-9	1.75e-9	2.48e-9

$$\sigma_E = \frac{E_0}{D_0}\sqrt{A_D - A_V}, \quad \sigma_I = \frac{E_0}{D_0 ek}\sqrt{B_V},$$

$$\sigma_B = \sqrt{B_\beta \beta_x^0}, \quad \sigma_R = \sqrt{A_D - \sigma_B^2},$$

$$B_\beta = \sigma_I^2(\beta_y^0 + 0.25L^2\gamma_y^0 - L\alpha_y^0)^{-1}$$

σ_E	σ_I	σ_B	σ_R	ϵ_n
keV	μm	μm	μm	μm
5.948 ± 0.06	71.4 ± 3	31.4 ± 1.3	27.6 ± 1.5	0.42 ± 0.02

FIG. 14: The black circles with error bars at the left plot show the measured slice width σ_M for different dispersion values D. The black circles with error bars at the right plot show the measured slice width σ_M for different values of TDS voltage V. The blue dotted lines are obtained by the numerical fit to Eq.(9) and Eq.(8).

Measurement with energy scan method

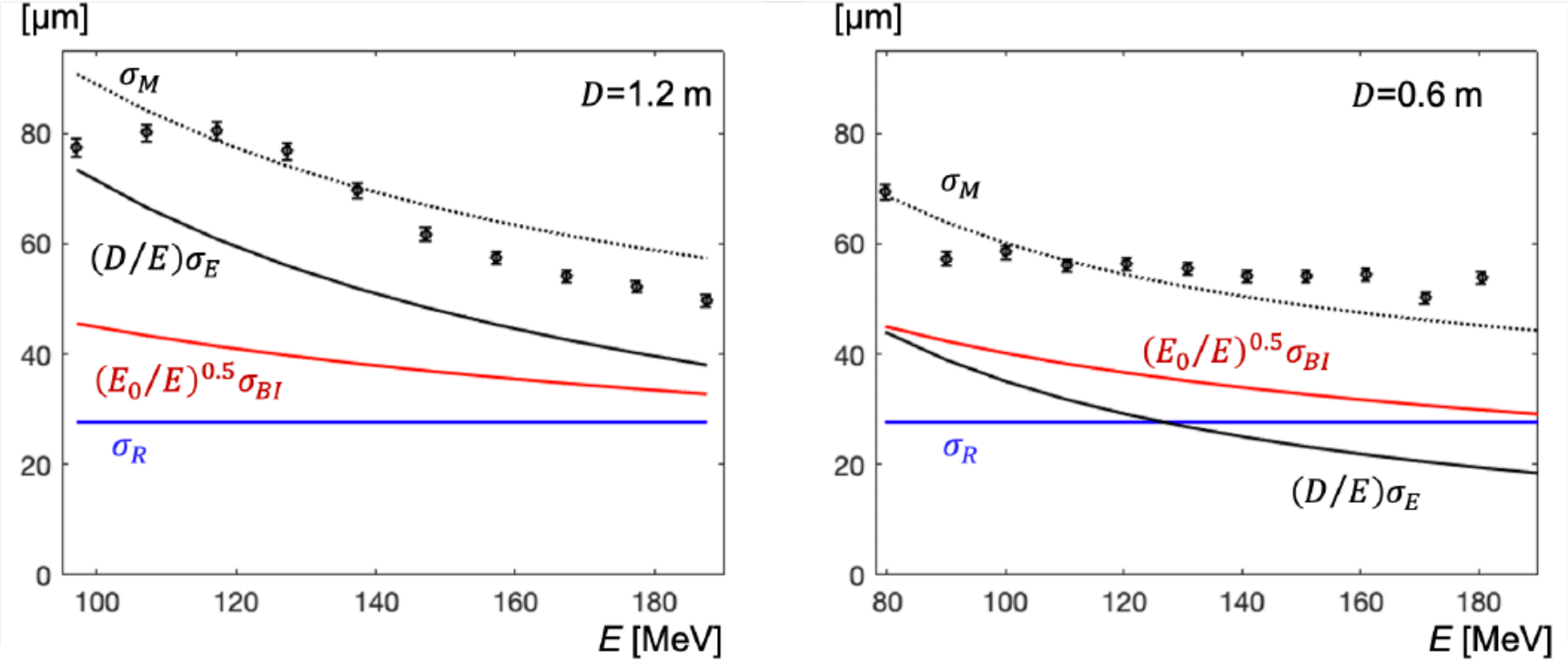

- The RF focusing in A1 depends on energy
- Matching to the optics was done at each energy
- The slice emittance changes
- The energy spread due to space charge and IBS changes

FIG. 15: Comparison of the measurements of the energy scan (dots with error bars) with the values calculated from the data of the dispersion scan

Validation of the experimental results

(1) $\sigma_E^0 = \frac{E}{D}\sigma_M$ - direct calculation at 130 MeV gives 7.9 keV.

(2) The energy spread estimation based on Eq.(10) uses only coefficient A_V and A_D. But there is another equation

$$\sigma_E = \frac{E_0}{D_0}\sqrt{D_0^2 B_D - V_0^2 B_V}, \qquad (13)$$

based on two other coefficients, B_D and B_V, from the numerical fits. From Eq.(13) we obtain that the energy spread is equal to 5.946 keV that agrees with the previous estimation (see Table V) with accuraccy 0.03%.

Validation

- (3)

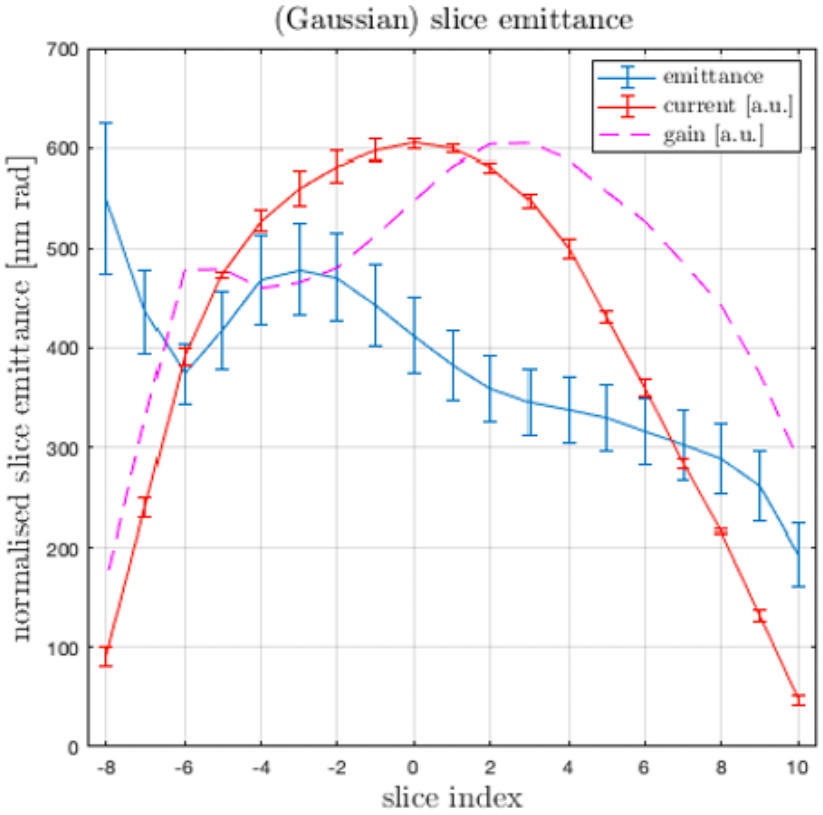

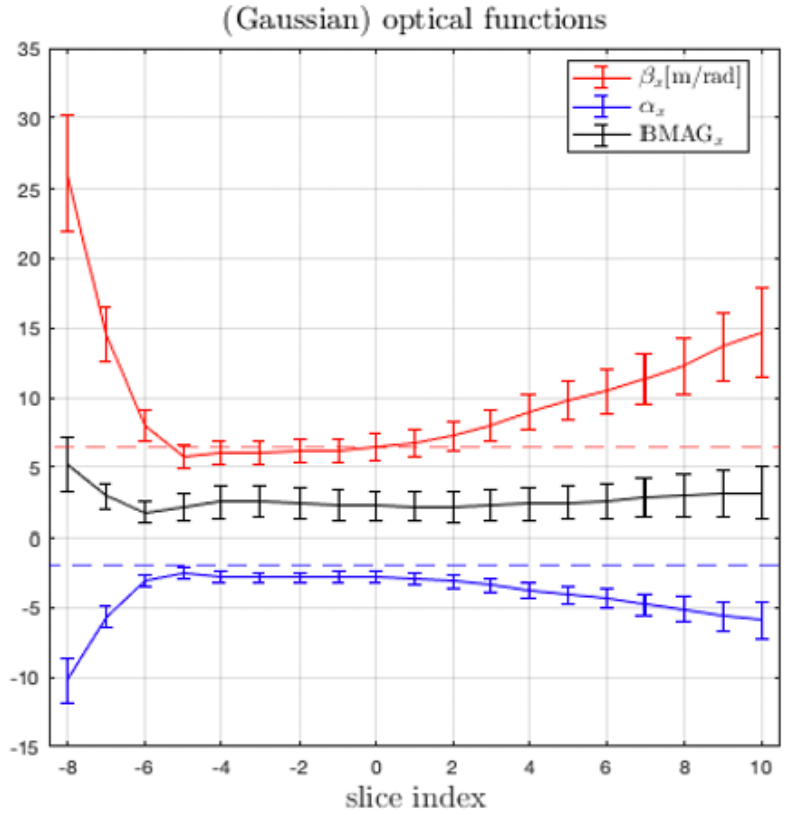

In order to check the estimation of the emittance ϵ_n we have done an independent measurement of the slice emittance with the standart tools [12] used by operators of the facility. The reults of independent measurement of the slice emittance are shown in Fig. 16 and the emittance of the central slice (slice index 0) agrees with the value listed in Table V.

Validation of the experimental results

(4) We had additional possibility to do the measuremt of the slice energy spread with the laser heater tuned for maximal SASE radiation energy. We have found that the energy spread in the electron bunch was 7.5 ± 0.1 keV.

In theoretical studies of microbunching carried out by our colleague M. Dohlus (see, for example, [13]) the optimal energy spread after laser heater for microbunching supression is nearly 8 keV. This number agrees reasonable with the measured one.

Discussion

The theoretical calculations with different numerical models predict the uncorrelated energy spread below 1 keV. The discrepancy between the theoretical estimations and the measurements could be caused by neglecting of full physics in the simplified numerical models. For example, it could be that the emission process from the cathode should be simulated differently. Additionally we do not take into account the intrabeam scattering and wakefields in the RF gun cavity. The number of macroparticles used in the simulations does not allow to take into account the microbunching during the transport from the gun to the OTR screen.

The energy spread from the RF gun measured at the European XFEL for charge of 250 pC is 5.9 ± 0.1 keV. This number is approximately 3 times lower then the energy spread of 14.8±0.6 keV reported recently by SwissFEL for the bunch charge of 200 pC [4] . The both guns use cesium telluride cathodes and the larger difference between these results requires additional efforts to understand.

Discussion: intrabeam scattering

S Di Mitri et al, Experimental evidence of intrabeam scattering in a free-electron laser driver, New J. Phys. 22 (2020) 083053

Z. Huang, Intrabeam Scattering in an X-ray FEL Driver, SLAC-TN-05-026, 2002.

$$\sigma_\gamma^2 = (\sigma_{\gamma 0}^2) + \frac{2r_e^2 N_b}{\langle\sigma_x\rangle \varepsilon_x^n \sigma_z}\Delta s$$

$Q = 250$ pC
$\varepsilon_x^n = 0.42\ \mu$m
$\sigma_z = 1.2$ mm
$\langle\sigma_x\rangle = 0.13$ mm
$\Delta s = 41$ m

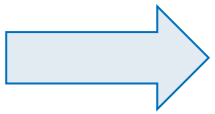

$\sigma_{E,IBS} = 2$ keV

Summary

- We have considered two methods for measurement of the uncorrelated energy spread in the injector section of the European XFEL
- For our setup the dispersion scan method is accurate and easy to carry out in the experiment
- For our setup we have not managed to obtain accurate results from the energy scan method
- The energy spread of 5.9 keV is almost three times smaller as the one measured for 200 pC at SwissFEL. However, it is still several times larger than one predicted by theoretical models.

"Although at present the handling of computers has become generally available and has become much simplified, before attempting to solve a problem, one should carefully think about whether it should be solved on a computer. Perhaps, through simplifications, it is possible to obtain an approximate answer that will satisfy the needs of practice. In any case, it must be remembered that solving complex problems on a computer is a difficult matter, requiring a large expenditure of energy from a person, both physical and moral."

K.I. Babenko

Acknowledgments

The authors thank M. Dohlus and M. Krasilnikov for helpful discussions. We thank members of the European XFEL team for providing help and conditions to carry out the measurements.